SUPPLEMENTAL FIGURES

A.

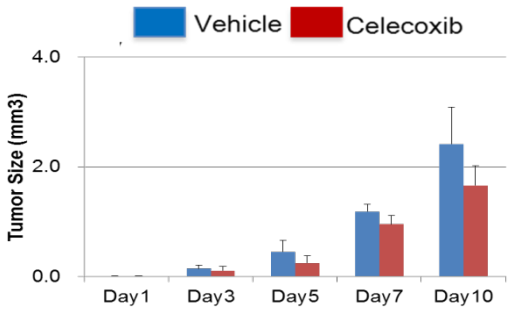

WT N=5

Celecoxib N=5

N.S.

B.

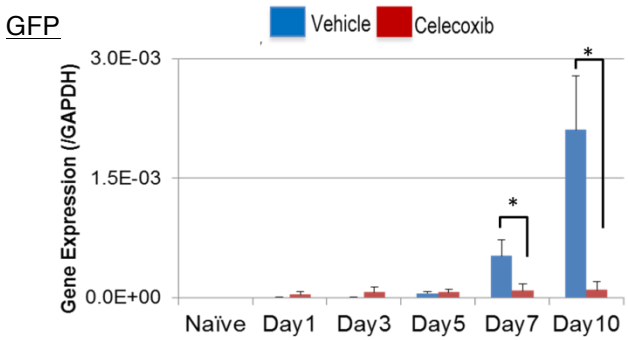

WT N=5

Celecoxib N=5

p< 0.05

C.

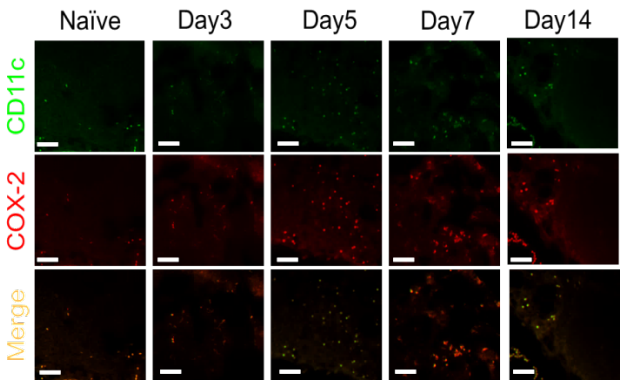

D.

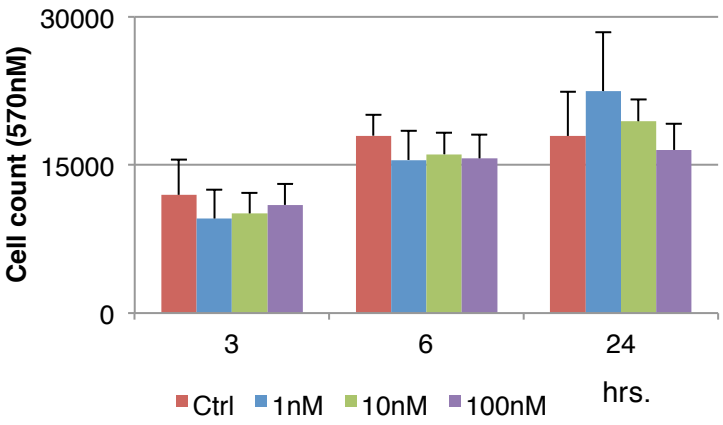

N.S.

Figure S1

A.

COX-2

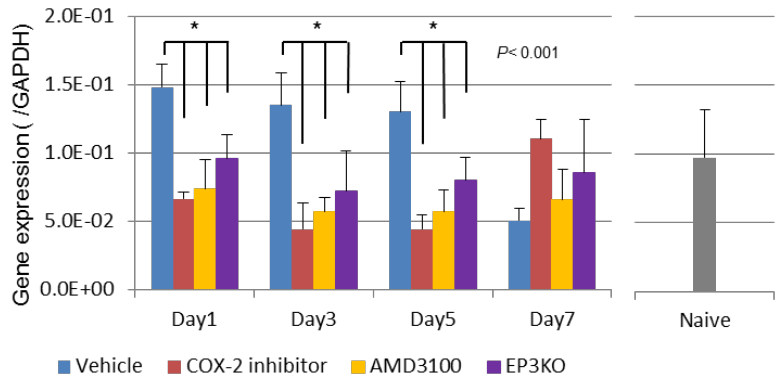

WT N=5
Celecoxib N=5
AMD3100 N=5
EP3KO N=3

B.

SDF-1

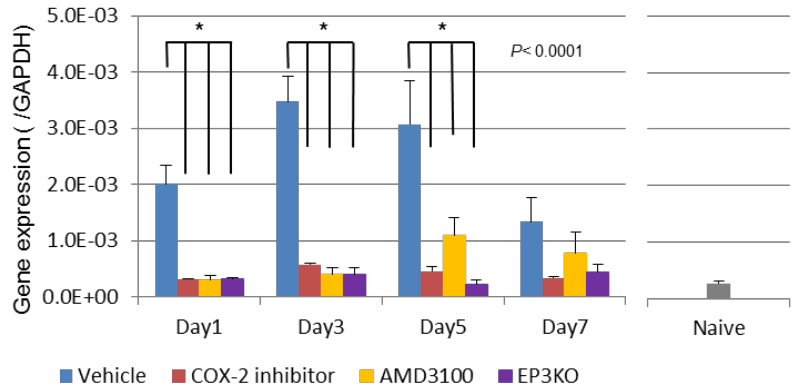

WT N=5
Celecoxib N=5
AMD3100 N=5
EP3KO N=3

C.

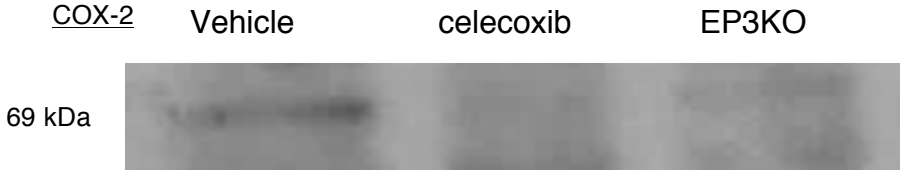

D.

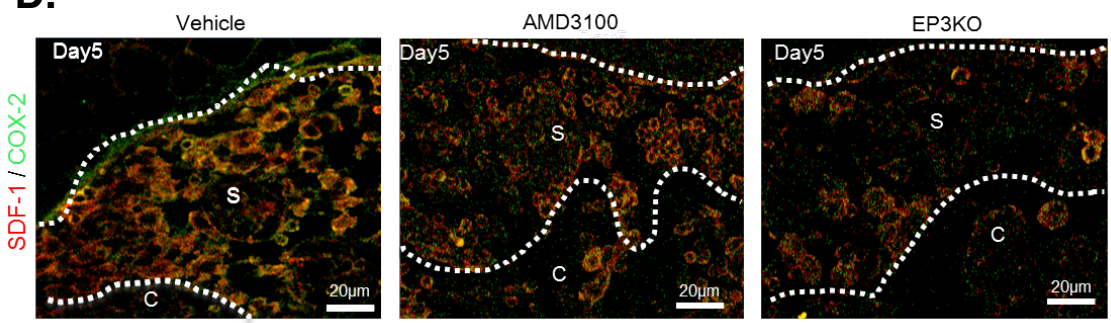

Figure S2

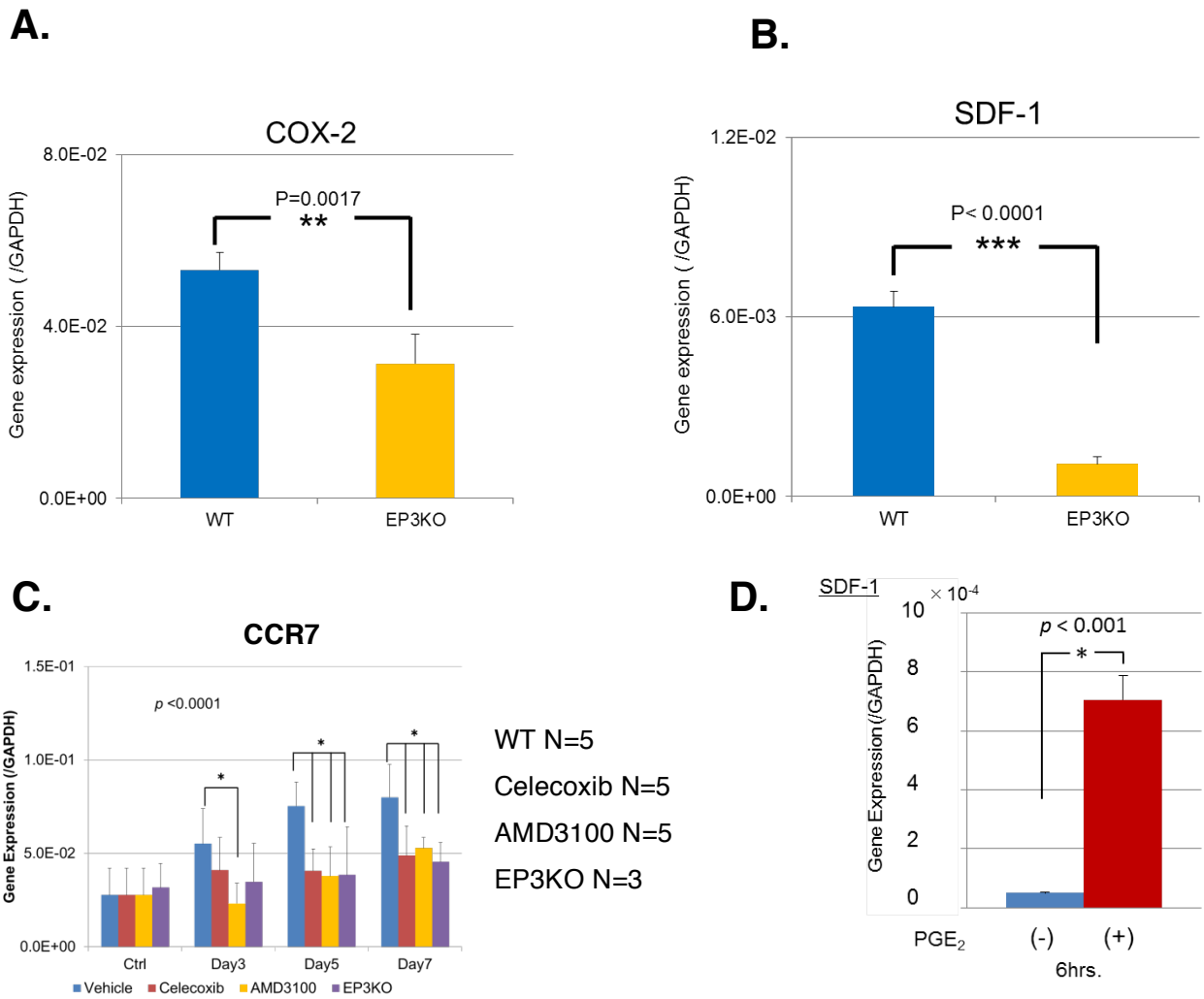
A.
COX-2
8.0E-02
4.0E-02
0.0E+00
Gene expression (/GAPDH)
P=0.0017
**
WT
EP3KO
B.
SDF-1
1.2E-02
6.0E-03
0.0E+00
Gene expression (/GAPDH)
P< 0.0001
***
WT
EP3KO
C.
CCR7
1.5E-01
1.0E-01
5.0E-02
0.0E+00
Gene Expression (/GAPDH)
p <0.0001
Ctrl
Day3
Day5
Day7
Vehicle
Celecoxib
AMD3100
EP3KO
WT N=5
Celecoxib N=5
AMD3100 N=5
EP3KO N=3
D.
SDF-1
× 10-4
10
8
6
4
2
0
Gene Expression (/GAPDH)
p < 0.001
PGE2
(-)
(+)
6hrs.
E.
.25
0.20
0.15
0.10
0.05
0.00
SDF-1concentration (ng/ml)
p= 0.11
p= 0.03
p= 0.59
PGE2
(-) (+)
0hrs
3hrs
6hrs
F.
0.2
0.15
0.1
0.05
0
SDF-1concentration (ng/ml)
p = 0.015
p = 0.022
EP agonist
(-)
EP1
EP2
EP3
EP4
3hrs
6hrs

Figure S3

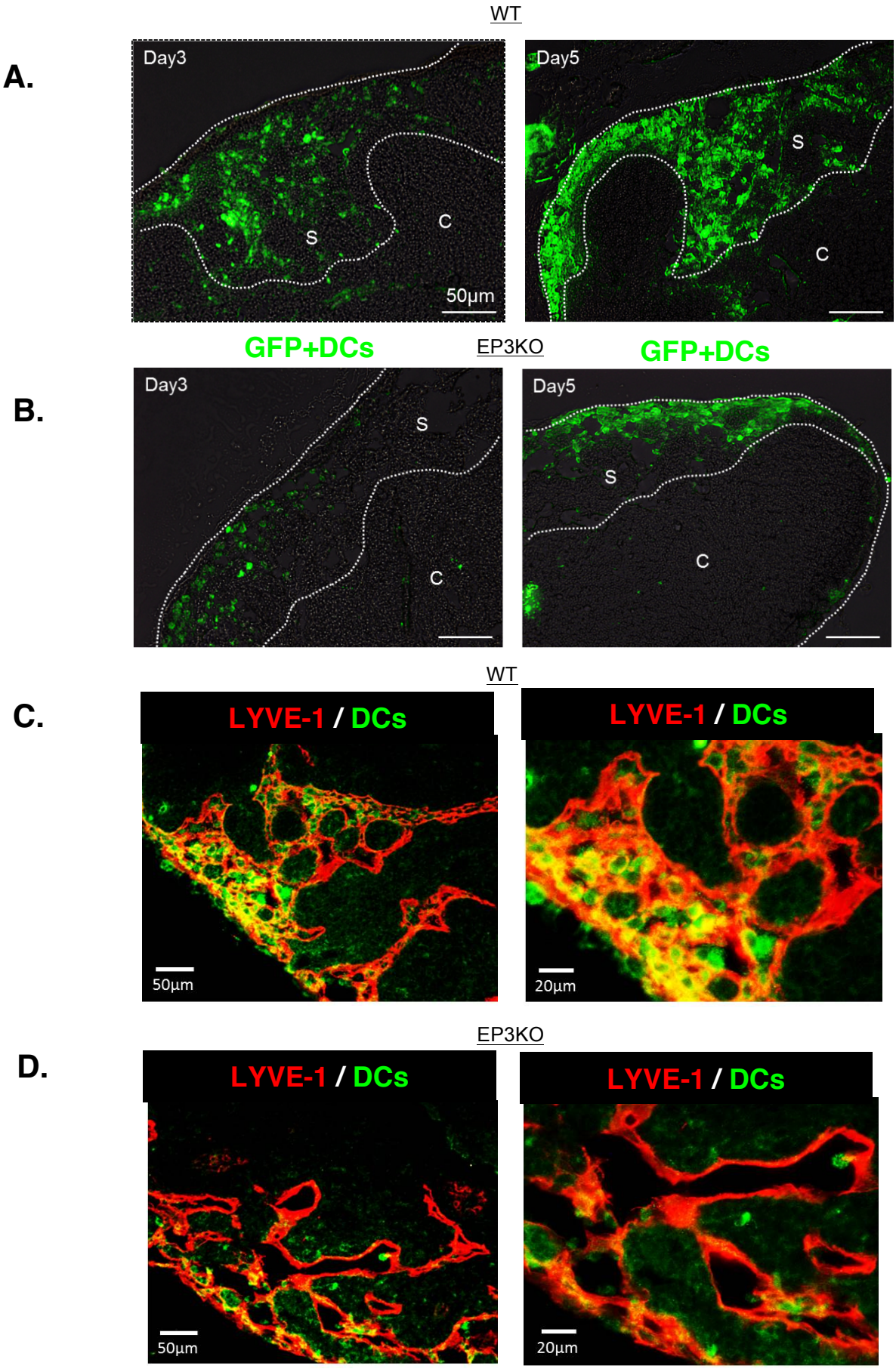
WT
A.
Day3
S
C
50μm
Day5
S
C
GFP+DCs
EP3KO
GFP+DCs
B.
Day3
S
C
Day5
S
C
WT
C.
LYVE-1 / DCs
50μm
LYVE-1 / DCs
20μm
EP3KO
D.
LYVE-1 / DCs
50μm
LYVE-1 / DCs
20μm

Figure S4

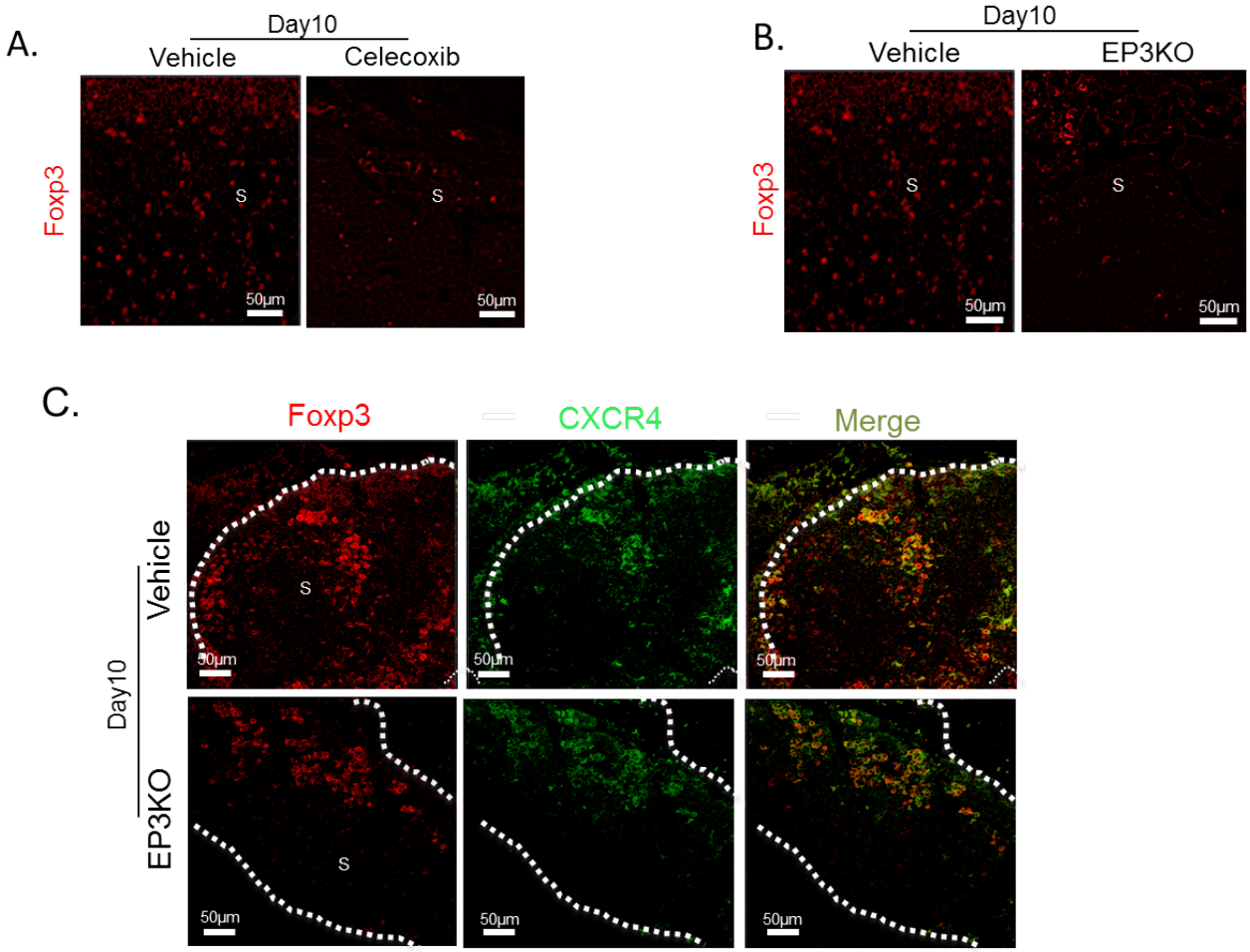
A.
Day10
Vehicle
Celecoxib
Foxp3
S
50μm
B.
Day10
Vehicle
EP3KO
Foxp3
S
50μm
C.
Foxp3
CXCR4
Merge
Day10
Vehicle
EP3KO
S
50μm

Figure S5

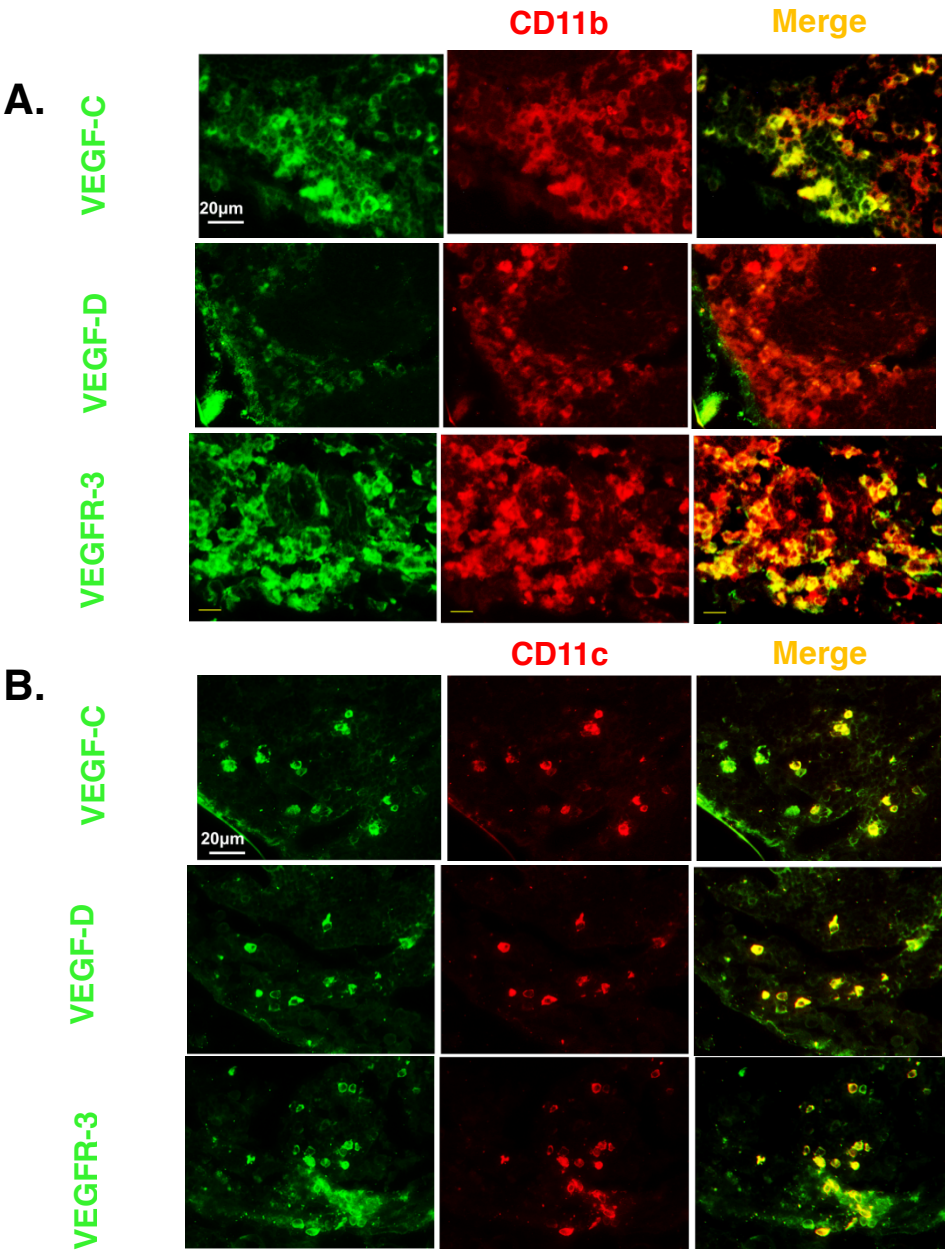
A.
CD11b
Merge
VEGF-C
VEGF-D
VEGFR-3
20μm
B.
CD11c
Merge
VEGF-C
VEGF-D
VEGFR-3
20μm

Figure S6

A.

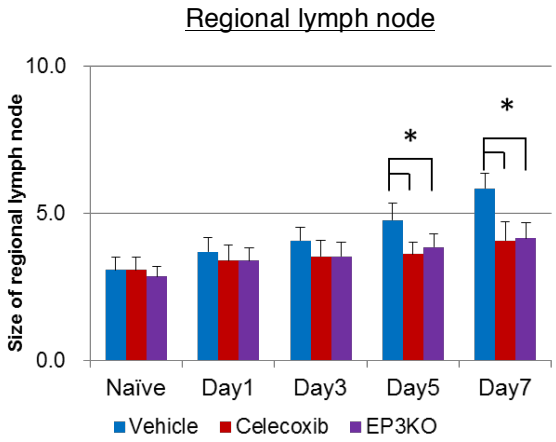

WT N=5

Celecoxib N=5

EP3KO N=3

p< 0.01

B.

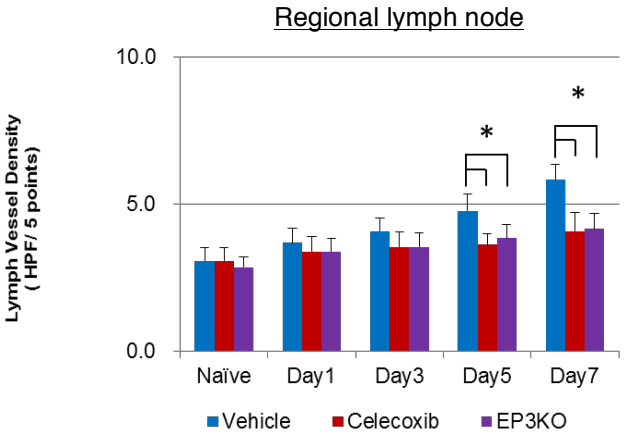

WT N=5

Celecoxib N=5

EP3KO N=3

p< 0.001

C.

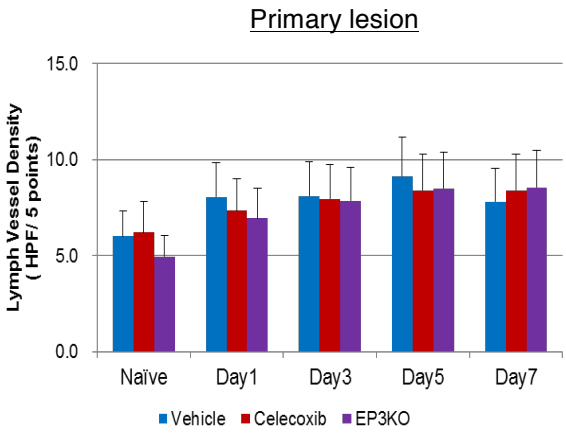

WT N=5

Celecoxib N=5

EP3KO N=3

N.S.

Figure S7

LEGENDS FOR SUPPL. FIGURES

Figure S1. COX-2 inhibitor treatment does not affect the progression of the primary tumor in the early phase before regional lymph node metastasis.

(A) Temporal changes in primary tumor growth after injection of LLC cells into the lungs. There was no significant difference (ANOVA) in primary tumor size between vehicle and celecoxib treated group (100 mg/kg/day).

(B) The expression of GFP at regional lymph node was not detected in early phase, but, in late phase, GFP was detected and there was significant difference between vehicle treated mice and celecoxib treated mice.

(C) The expression of COX-2 and CD11c with only matrigel injection. These factors increase slightly at regional lymph node. Day 7. Bars; 50μm

(D) In virto, we investigated the effect of celecoxib on LLC growth with MTT assay. There was no significant inhibition in growth rate with celecoxib treatment.
Error bars indicate the mean ± SD.

Figure S2. SDF-1 induction in regional lymph nodes is essential for premetastatic niche formation.

(A) The expression of COX-2 analyzed by RT-PCR. COX-2 expression in regional lymph nodes suppressed in celecoxib and AMD3100 treated mice and EP3KO mice compared to vehicle treated mice.

(B) The expression of SDF-1 analyzed by RT-PCR. SDF-1 expression in regional lymph nodes suppressed in celecoxib and AMD3100 treated mice and EP3KO mice compared to vehicle treated mice.

(C) Western blotting of COX-2 at regional lymph node. The expression of COX-2 (69kDa) was detected in vehicle treated mice, but it was inhibited in celecoxib treated mice and EP3KO mice.

(D) Immunofluorescence images of COX-2/SDF-1 expression in regional lymph nodes at day 5 post-injection of LLC cells. COX-2/ SDF-1 double positive cells accumulated in the subcapsular regions at day 5 before the arrival of GFP-negative LLC cells. AMD3100 treatment inhibited the accumulation of double positive cells. Accumulation of the double positive cells was reduced in EP3 KO mice compared with that in WT mice. Bars; 20μm. S; subcapsular regions, C; cortical regions.

Figure S3. The function of DCs induced to premetastatic site and effect of PGE_2 and EP agonists on the expression and secretion of SDF-1 in cultured DCs.

(A) The expression of COX-2 analyzed by RT-PCR in FACS-sorted CD11c+DCs from regional lymph node day 5 after LLC implantation. COX-2 expression in DCs in regional lymph nodes was suppressed in EP3KO mice compared to vehicle treated mice. N=5.

(B) The expression of SDF-1 analyzed by RT-PCR in FACS-sorted CD11c+DCs from regional lymph node day 5 after LLC implantation. SDF-1 expression in regional lymph nodes was suppressed in EP3KO mice compared to vehicle treated mice. N=5.

(C) The expression of CCR7 by RT-PCR analysis at regional lymph node was suppressed in celecoxib treated mice compared to vehicle treated mice.

(D) Addition of PGE_2 (0.01 nM) increased the expression of SDF-1 in cultured dendritic cells. RT-PCR was performed with SDF-1 primers as described in the supplemental methods. N=6. $P < 0.05$ (Student's t-test).

(E) Time-course of SDF-1 secretion by cultured dendritic cells stimulated with PGE_2 (0.01 nM). The concentration of SDF-1 in the culture medium was determined by ELISA. N=6. $P < 0.05$ (Student's t-test).

(F) Time-course of SDF-1 secretion by cultured dendritic cells stimulated with specific EP receptor agonists (0.01 nM). The concentration of SDF-1 in the culture medium was determined by ELISA. N=6. $P < 0.05$ (Student's t-test)
Error bars indicate the mean $\pm$ SD.

Figure S4. i.v.-injected DCs were recruited to premetastatic sites in a PGE_2-EP3 signaling-dependent manner

(A) Immunofluorescence images showing DCs isolated from bone marrow from GFP transgenic WT mice intravenously-injected to regional lymph nodes at day 3 and day 5 after LLC implantation. Bars; 50 μm.

(B) Immunofluorescence images showing DCs isolated from bone marrow from GFP transgenic EP3KO mice intravenously-injected to regional lymph nodes at day 3 and day 5 after LLC implantation. DCs recruited to subcapsular region on EP3 signaling dependent. Bars; 50 μm.

(C, D) Immunofluorescence images show by IHC with LYVE-1 at Day 10 after LLC injection. GFP^+DCs from EP3KO (D) was inhibited the accumulation to pre-metastatic site compared to GFP^+DCs from WT (C). Bars; 50μm (left), 20μm (right).
S; subcapsular region. C; cortical region

Figure S5. Recruitment of Tregs to the regional lymph nodes was regulated by COX-2 derived PGE_2-EP3 signaling and effect of Tregs recruitment on tumor metastasis

(A) Immunofluorescence images showing Foxp3 in the subcapsular regions of regional lymph nodes at day 10. Celecoxib treatment reduced the accumulation of Foxp3-positive cells.

(B) Immunofluoroscence images showing Foxp3 in the subcapsular regions of regional lymph nodes at day 10. EP3 KO mice showed reduced accumulation of Foxp3-positive cells compared to WT mice. Bars; 50 μm.

(C) Immunofluorescence images showing Foxp3/CXCR4 double positive cells in the regional lymph nodes after LLC injection at day 10. The accumulation of

Foxp3/CXCR4 double positive cells in the subcapsular regions was reduced in EP3KO mice compared with that in WT mice. Bars; 50 μm.
S; subcapsular region. C; cortical region

Figure S6. Double immunostaining of CD11b/CD11c and prolymphangiogenic factors in regional lymph nodes

(A) Immunofluorescence images showing prolymphangiogenic factors, such as VEGF-C, VEGF-D and VEGFR-3 in the subcapsular regions of regional lymph nodes. The positive cells are CD11b+ macrophages. Bars; 20 μm.

(B) CD11c+ DCs are also positive to the tested prolymphangiogenic factors. Bars; 20 μm.

Figure S7. The differences of lymph node size and lymph vessel density between vehicle treated mice and celecoxib treated mice/EP3KO mice.

(A) Lymph node size after LLC injections. There were significant differences between vehicle treated mice and celecoxib treated mice/EP3KO mice at day 5 and day 7.

(B) In regional lymph node, there was also significant difference in lymph vessel density after injection between vehicle treated mice and celecoxib treated mice/EP3KO mice at day 5 and day 7.

(C) In primary lesion, there was no significant difference of lymph vessel density.
Error bars indicate the mean $\pm$ SD.

SUPPLEMENTAL EXPERIMENTAL PROCEDURES

Western blotting

Total cellular proteins were isolated using radioimmunoprecipitationassay buffer [50 mmol/L Tris-HCl (pH 7.2), 1% Nonidet P-40, 0.5% sodium deoxycholate, 0.1% sodium dodecyl sulfate]. Nuclear and cytoplasmic fractions were also prepared using NE-PER nuclear and cytoplasmic extraction reagents (Pierce; Thermo Fisher Scientific). Aliquots of 1 to 10 mg of protein were resolved by SDS-PAGE and transferred to membranes. Immunoblotting was performed with goat anti-mouse COX-2 antibody (1:200) and rat anti-mouse SDF-1 (1:200; Santa Cruz Biotechnology), followed by incubation with donkey anti-goat horseradish peroxidase conjugated secondary antibody (1:200; Santa Cruz Biotechnology), and mouse anti-mouse horseradish peroxidase conjugated secondary antibody (1:200; GE Healthcare). The protein was visualized by a commercial chemiluminescent method with an Amersham ECL detection system (GE Healthcare).

Flow Cytometric Analysis

Five days after tumor implantation, regional lymph nodes were harvested. The lymph nodes were treated with 5% collagenase for 15 min to release dendritic cells in the medium. The collected cells were stained with PE-labeled anti- CD11c Ab, and the cells were then fixed and permeabilized using the intracellular staining kit (Foxp3 Fixation/Permealization buffer (eBioscience, 00-5521-00), IntraStain, Fixation and Permeabilization Kit for Flow Cytometry(DAKO, K2311)) before staining of COX-2 or SDF-1. For COX-2 or SDF-1 staining, we used rabbit polyclonal antibody to mouse COX-2 from Cayman (Ann Arbor, Michigan) or anti-human/mouse SDF-1 monoclonal antibody from R&D Systems Inc. (Minneapolis, Minnesota), respectively, which was the only fluorescein-labeled Abs applicable to flow cytometry analyses.

MTT Assay

Single cell suspensions were obtained by mechanical disaggregation of the floating cell line and by trypsinization of monolayer cultures. The assay is dependent on the cellular reduction of MTT (Sigma Chemical Co., St. Louis, MO) by the mitochondria dehydrogenase of viable cells to a blue formazan product which can be measured spectrophotometrically. Following appropriate incubation of cells, with or without drug, 0.1 mg (50 nl of 2 mg/ml) MTT was added to each well and incubated at 37°C for a further 4 h before processing as described below. To determine the relationship of cell number to MTT formazan crystal formation increasing cell numbers 10,000/well were plated, using LLCs. MTT was immediately added and plates were incubated for 4 hrs. Plates were then processed as described and absorbance was determined. For cell growth studies, serially increasing cell numbers were plated in different columns across 96-well plates. Actual cell number was measured daily by removing cells from individual wells at each cell concentration. Cell counts were performed using a panicle counter, with all measurements carried out in triplicate. Identical plates were processed daily using MTT, measuring absorbance with a

scanning multiwell spectrophotometer (multiplate reader; SoftMax Pro, Molecular Devices, Inc., California, USA).

Growth rates varied between the cell lines used; therefore, the number of cells plated was adjusted so that untreated cells were in exponential growth phase at the time of harvest.

Assays were performed using continuous exposure to celecoxib, 0.01nM, 0.1nM and 1nM, for 3h, 6h and 24h. For continuous exposure studies, equal numbers of cells were inoculated into each well in 0.18 ml of culture medium, to which 0.02 ml of lux concentrated drug or phosphate-buffered saline was added. Drugs and cells were mixed, and following incubation, cells were centrifuged at 12,000 rpm for 5 min, washed twice with phosphate-buffered saline, and then plated directly into plates. Following incubation the media from plates containing adherent cells was aspirated completely. The majority of the media was then aspirated, taking care not to disturb the formazan crystals, leaving approximately 30 pi of media in each well. All results represent the average of a minimum of 8 wells. Additional controls consisted of media alone with no cells, with or without the various drugs.